AAS 05-110

EXPLORATION OF DISTANT RETROGRADE ORBITS AROUND EUROPA

Try Lam* and Gregory J. Whiffen†

This paper explores the applications of Distant Retrograde Orbits (DROs) around Europa, a class of orbit which can be stable for a very long time. These orbits exist due to a larger perturbation from Jupiter, and are of particular interest due to proposed missions such as NASA's Jupiter Icy Moon Orbiter (JIMO). Preliminary investigation has found DROs to be ideal quarantine orbits due to their long-term stability and their existence at a large range of distances away from Europa. The paper also demonstrates that continuous families of DROs provide instantaneously stable transfer paths for both escape and capture around Europa.

INTRODUCTION

The behavior and applications of Distant Retrograde Orbits (DROs) are explored around Europa. Such orbits are of particular interest due to proposed missions such as NASA's Jupiter Icy Moon Orbiter (JIMO). At low altitudes Europa's gravity field cause a secular drift in eccentricity, which rapidly leads to collision with the surface. At higher altitudes, the third-body perturbations from Jupiter dominate, and can lead to collision or escape after a few revolutions. In this dynamically chaotic region it becomes difficult to design stable science orbits and transfers to and from them.

As an end-of-mission option, DROs are ideal quarantine orbits because of their long-term stability (hundreds of years) and the low relative propellant cost of transferring to them. DROs compare favorably to alternate solutions, such as impacting Jupiter or escaping the Jovian system. Understanding DROs also allows mission designers to design stable transfers to and from science orbits. DROs are useful for transfer design due to the existence of small highly inclined DROs and due to their natural continuation to low altitude circular retrograde orbits. Key characteristics that are being investigated are their dynamics, their long-term stability, and the cost of transferring between low altitude orbits and DROs.

As the name suggests, DROs are distant retrograde orbits, and they exist due to gravitational perturbation of a third body, but we will later see that they exist at small ranges as well. DROs have been studied in depth over the past 40 to 50 years using the Planar Circular Restricted Three-Body Problem (PCR3BP) and Hill's Problem. Individuals who have contributed to the understanding of periodic orbits include Hénon (Ref. 1 & 2), Benest (Ref. 3), Stromgrën (Ref. 1), and Broucke (Ref. 4). The literature provides classifications and nomenclature to describe this family of orbits.

* Associate Member of Engineering Staff, Outer Planet / Small Body Flight Dynamics Section, Jet Propulsion Laboratory, California Institute of Technology, Pasadena, CA 91109, Member of AIAA
† Senior Member of Engineering Staff, Outer Planet / Small Body Flight Dynamics Section, Jet Propulsion Laboratory, California Institute of Technology, Pasadena, CA 91109, Member of AIAA

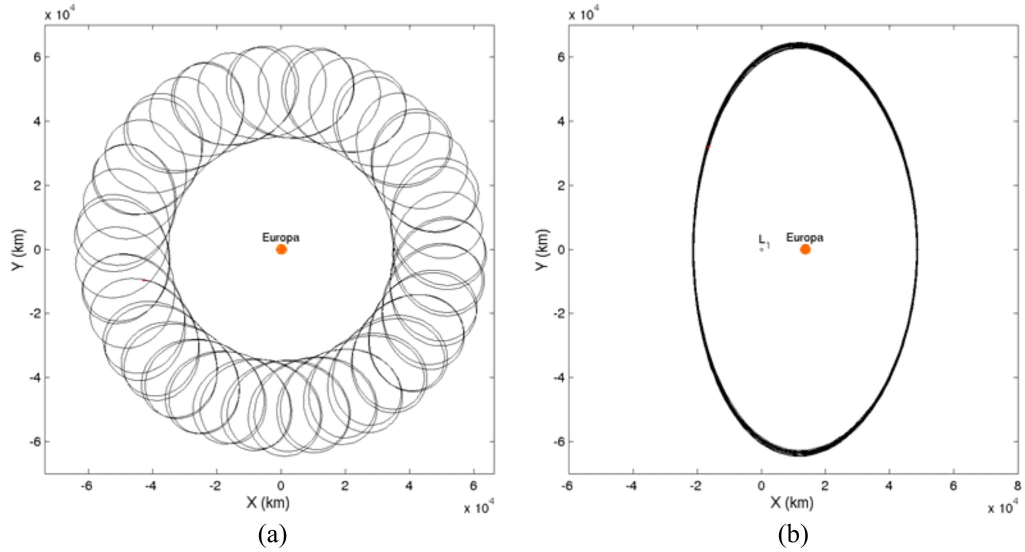

Figure 1 A 35,000 km DRO (x-axis) about Europa in the inertial frame (left) and the corresponding orbit in the L1-centerd rotating frame (right). Note that the smaller DRO axis in the rotating frame is the corresponding close-approach points in the inertial coordinates, while the larger axis of the DRO corresponds to the outer portion of the orbit in the inertial coordinate system. In both plots the direction of orbit is retrograde although Figure 1a has periodic spirals that oscillates between the retrograde and the prograde (or direct) directions.

In the inertial frame, the general motion of a DRO is retrograde with smaller periodic oscillations or loops that cause the motion of the spacecraft to oscillate between retrograde and direct motion as it proceeds around Europa (Figure 1a). Due to this motion, DROs cannot be described in terms of classical orbital elements. In the rotating frame, with one axis fixed along the Jupiter-Europa line, DROs appear to be retrograde imperfect ellipses with a "semi-minor" axis along the Jupiter-Europa line (Figure 1b and 2). In the asymptotic case of more energetic (larger) orbits these elliptical DROs have approximately a 2:1 axis

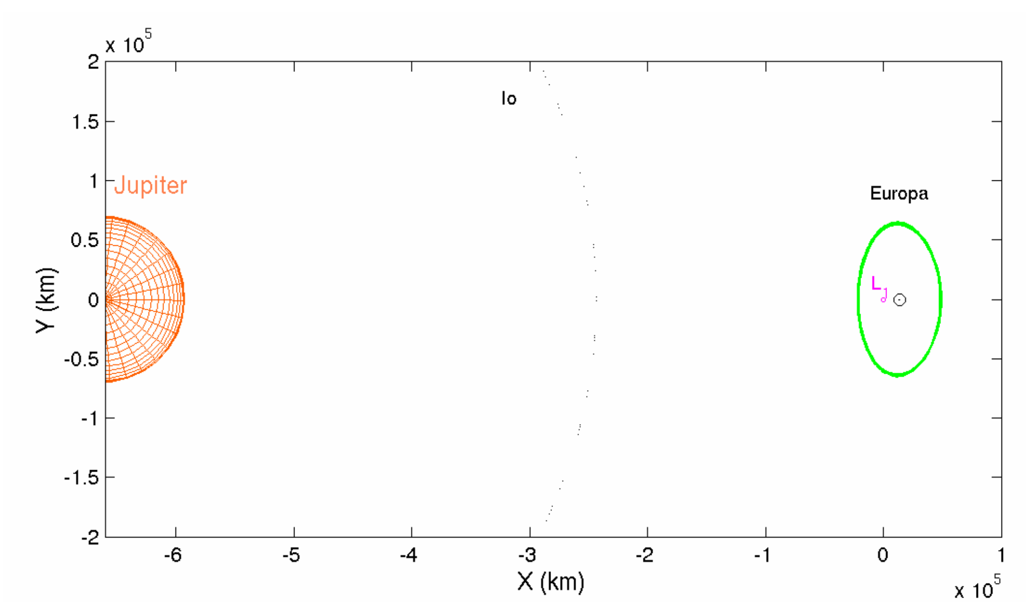

Figure 2 A 35,000 km (x-axis) DRO about Europa in the rotating frame (centered at L1)

ratio, while at smaller distances (approximately half the distance to L1) the orbits are near circular in shape and speed.

The benefit of DROs in comparison to other periodic orbits, especially as potential quarantine orbits, is stability. Extensive work done by Hénon and Benest has shown that simple-period planar DROs (which they classified as family *f*) are stable in Hill's approximation. There is an exception to the previous statement; there are two specific orbits from the entire family of DROs that are unstable due to another family of period-three orbit (Figure 3, called family g3 by Hénon) intersecting the family *f* twice in phase space (Ref. 1 & 2). Period-three orbit are orbits that close or repeat after three revolutions around Europa. The period-three orbit causes instability to the family of DROs due to its resonance with Europa's period (Ref. 3). Stability of DROs will be further discussed in the Stability section of this paper, and the influence of family g3 on the stability of DROs will be evident. Benest later showed that regions of stability exist for all ranges of mass ratios as well, but pockets of instability develop in regions where it was predominantly stable in Hill's case (Ref. 3, 5 & 6), which is consistent with Broucke's and Bruno's work (Ref. 4 & 6).

This paper will also discuss preliminary results for transfers between DROs and Europa's science orbit, and will discuss the benefit of modeling a DRO's profile for stable transfers.

Nearly all the analysis done in this paper was done numerically with Mystic, JPL's high fidelity low-thrust trajectory optimization tool developed by Gregory Whiffen and collogues, but occasionally we resort to numerical analysis using Hill's approximation for comparison purposes. Mystic is based on the Static/Dynamic Optimal Control algorithm (Ref. 7). Extensive analytical work on DRO type orbits, their transfers, and orbital stability in the multi-body problem in general can be found from works by Szebehely (Ref. 8), Broucke, Hénon, Benest, Scheeres (Ref. 9), Ocampo, and others. The benefit of using Mystic is that it has allowed us to numerically analyze (and optimize when possible) dynamically complex trajectories and transfers with JPL's ephemerides and to validate many of the works done by the individuals above.

EQUATION OF MOTION AND ORBIT CHARACTERIZATION

The majority of the analyses on DROs and related families in the literature are based on the planar circular restricted three-body problem (PCR3BP) and Hill's model. In Hill's approximation it is assumed that $\mu \sim 0$, where μ is defined as

$$\mu = \frac{M_1}{M_1 + M_2} \tag{1}$$

where M_1 is the mass of Europa and M_2 is the mass of Jupiter. For Jupiter and its moons this is fairly accurate, since $\mu_{\text{Jupiter-Europa}} = 0.0000252803$. Centering about Europa Hill's equations are written as

$$\begin{pmatrix} \ddot{\xi} \\ \ddot{\eta} \end{pmatrix} = \begin{pmatrix} 2\dot{\eta} \\ -2\dot{\xi} \end{pmatrix} + \begin{pmatrix} 3\xi \\ 0 \end{pmatrix} - \frac{1}{r^3}\begin{pmatrix} \xi \\ \eta \end{pmatrix} \tag{2}$$

where ξ is the rotating x-axis fixed along the line from Europa to Jupiter and η is the rotating y-axis, which is perpendicular to the ξ axis. For these set of equations the Jacobi constant is defined as

$$\Gamma = 3\xi^2 + \frac{2}{r} - \dot{\xi}^2 - \dot{\eta}^2 \tag{3}$$

where $r = (\xi^2 + \eta^2)^{1/2}$ and is the distance from M_2 to the satellite. Note that as $\Gamma \rightarrow -\infty$, the orbit's Jacobi energy increases. Therefore, larger DROs have larger energies.

In this paper (X, Y) and (ξ, η) will be used interchangeably, and plots and figures generated based on Hill's approximation were done using Hill's equations, Eq. (2). Plots based on Hill's approximation can be distinguished from plots created by Mystic (ephemeris) by their lack of physical units. Orbits based on the JPL "real" ephemeris can never be exactly periodic. As long as orbits using a real ephemeris are nearly periodic, we will refer to them simply as "periodic".

Periodic Orbits

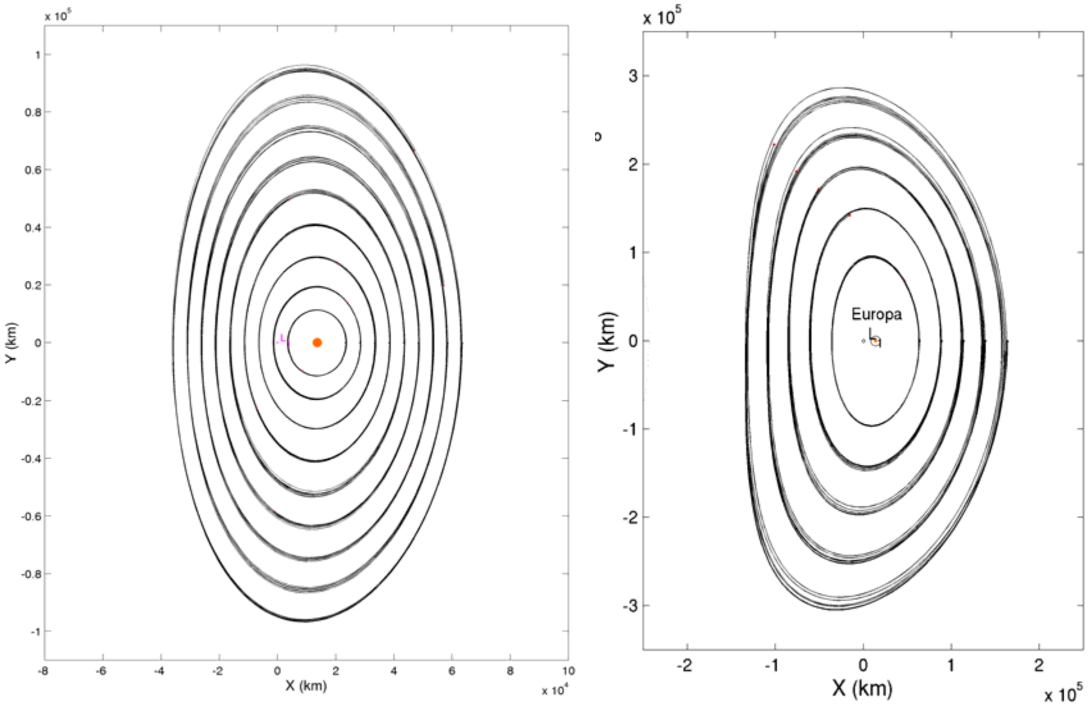

(a) (b)

Figure 4 Europa's family of near periodic Distant Retrograde Orbits (DROs) numerically integrated with Mystic for 20 days and centered in the rotating frame. Gravitating bodies include the Sun, Jupiter, Io, Europa, Ganymede, and Callisto. (a) Sizes range from 10,000 km (innermost orbit) along the X-axis to 50,000 km in increments of 5,000 km. (b) Size ranges from 50,000 km to 150,000 km in increments of 25,000 km.

We studied periodic DROs around the Jovian moons. Close to the moons, DROs are indistinguishable from circular retrograde orbits dominated by two-body dynamics. For this reason we will not distinguish between what some may refer to as "true" DROs, which are very distant orbits, and small DROs. For larger DROs, the size of the Libration (L1 or L2) point distance, Jupiter's gravitational forces dominate and a three-body model cannot be avoided. For very large DROs a distortion appears in the "ellipse" and the tips along the major axis of the ellipse bend toward Jupiter (Figure 4).

Simple-periodic. In this paper the term DRO refers to simple-periodic symmetrical DROs about the rotating X-Z plane, "simple", meaning the periodic orbit crosses the rotating X-axis twice for every period. This is not to be confused with non-periodic DROs, or the librations of DROs, where multiple non-periodic crossings exist. "Simple-periodic" also means that there exist no periodic orbits that are of period-two or larger. Period-two and period-three periodic orbits are defined as orbits which orbit two and three times, respectively, before they close. These N-periodic DROs are usually orbits which bifurcate from the main sequence of simple-periodic DROs as we continue along the family of DROs in increasing energy in phase space.

As mentioned above DROs are classified in family *f*, a family of orbits that are part of the nine natural families (Ref. 1). Of the nine natural families Szebehely, Strömgren, Hénon define five families of simple-periodic symmetrical orbits: *a, c, f, g,* and *g'*. Families *a* and *c* are L_2 and L_1 Lyapunov orbits. Family *f* and *g* begin respectively as retrograde and direct orbits around the second body M_2 (in our case, Europa). Family *g'* branches or bifurcates from family *g*. This paper will only briefly introduced these other periodic families to assist in the understanding DROs and transfers to them. For more detail on periodic orbits in Hill's approximation see Henon (Ref 1).

In Hénon's studies of Hill's approximation, families of periodic orbits retain finite shape; they become either circular orbits (periodic solutions of the 1st kind in Poincaré's terminology), elliptical orbits (periodic solutions of the 2nd kind), or orbits with consecutive collisions (periodic solutions of the second species) (Ref. 10). The importance of these periodic orbits becomes evident in designing transfer trajectories to DROs due to their close approaches to M_2, which can be use as starting states to begin the transfer.

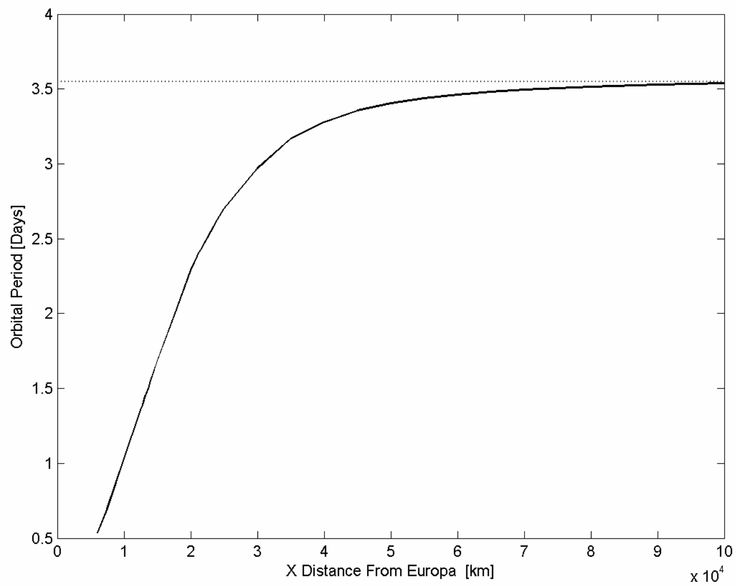

Figure 5 Orbital period of the Europa's DROs in the rotating coordinate system in days as a function of DRO X-axis size (km). Orbital period asymptotically approaches that of Europa about Jupiter, 3.55 days.

Mathematically, the simplest case of a DRO is one of the asymptotic forms of the family *f* as $\Gamma \rightarrow -\infty$ (higher energy orbits) where the attraction from Europa can be neglected in the first order approximation. If we restrict the problem to periodic orbits that are symmetric about the X-axis, the equation of motion for orbits of family *f* in Hill's approximation reduces to

$$\xi = K_1\cos(t), \qquad \eta = -2\,K_1\sin(t), \qquad \Gamma = -K_1^2 \tag{4}$$

See Henon's paper for detail (Ref. 1). The resulting orbit is exactly an ellipse with its center at M_2. Note that the axis ratio is 2:1 with a period of 2π, which is the orbital period of M_2 about M_1 (Europa's period about Jupiter ~ 3.5 days), in the retrograde direction. This orbit is simply the relative motion between an ordinary two-body circular orbit (Europa) and an ordinary two-body elliptical orbit (spacecraft) both about Jupiter and both with the same orbital period. Figure 5 shows orbital periods of DROs in the rotating coordinate system around Europa using the real ephemeris. Note that for large DROs, where the effect of Europa is negligible, the orbital period asymptotically approaches the orbital period of Europa about

Jupiter. From Eq. (4) an analytical approach in finding the abscissa of the intersection ξ_0 and the initial velocity $V\eta_0$ for values of Γ are

$$\xi_0 = -(-\Gamma)^{1/2} \tag{5}$$

$$V\eta_0 = -2\,\xi_0 \tag{6}$$

Note that ξ is the x-axis in the rotating coordinate system and η is the corresponding y-axis.

Other asymptotic forms exist for other periodic families. In Figure 6 we see the continuation of family *a* (L2 Lyapunov orbits) toward its asymptotic form, and note that unlike orbits in family *f* these families of orbits approach and eventually collide with Europa when $\Gamma \rightarrow -\infty$. For the near collision orbits, such as family *a*, these orbits can be used as transfer orbits to the DROs for high thrust missions. The collision orbits can be used as initial conditions for launch to large retrograde and direct orbits (Ref. 11 & 12). An interesting aspect of families *a* and *c* are that they are prograde near the vicinity of M_2 but are retrograde with respect to M_2 at its most distant locations, and may be good reference states for the transfer orbits.

Non-Periodic Orbits

Using the real ephemeris, or using the perturbed restricted three-body model, DROs are quasi-periodic. They do not exactly close on every orbit, but can come very close. In Hill's case, the quasi-periodic DROs follow a librating elliptical pattern where the ellipse oscillates along the Y-axis. In the ephemeris case and in the CR3BP the oscillation of the ellipse remains predominantly along the Y-axis, but the curvature of the ellipse becomes more evident as the orbit oscillates about an imaginary circumference (Europa's orbit about Jupiter).

In the quasi-periodic case, solutions of Hill's equation of motion (Eq. (4)) can be represented as set

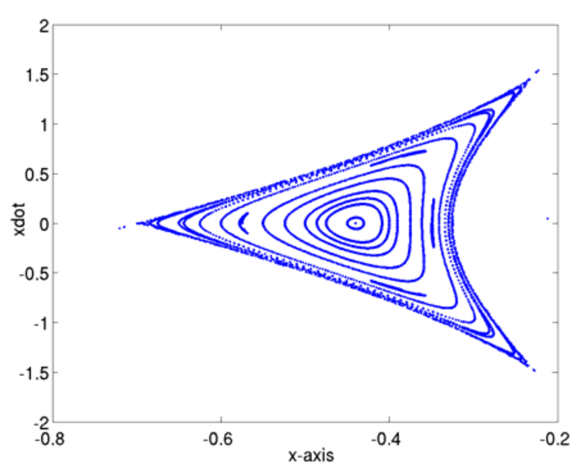

Figure 7 Poincaré Section with Γ = 1. Note the appearance of the period-three family *g3* at the three corners of the stability boundary region. X=0 is the location of Europa.

of points in a two-dimensional $(\xi,\dot{\xi})$ Poincaré section (Ref. 2). This is achieved by setting Γ to a fix Jacobi energy level and looking at the trajectory as it crosses Y=0. By doing so Eq. (3) is now of the form

$$\dot{\xi}^2 \leq 3\xi^2 + \frac{2}{|\xi|} - \Gamma \tag{7}$$

This method generalizes the all possible orbits which can exist for a fixed Γ, and expand from exclusively looking at periodic orbits to including quasi-periodic and chaotic orbit as well. Besides providing the capability of viewing four-dimensional trajectories in two-dimensions, this method is used to determine if orbits are stable by their repeated crossings. If an orbit is periodic then the Poincaré section will show a point or set of points that are not connected. If an orbit is quasi-periodic then the Poincaré section shows points which connect and form curves. If an orbit is unstable then the points are scattered. For example: Figure 7 shows a Poincaré section near Europa for Γ=1. At this energy level stable prograde orbits no longer exist and only retrograde orbits continue to exist. At the center of the triangular structure we note a "point" that represents a simple-periodic retrograde orbit, which is surrounded by quasi-periodic orbits. The structure in Figure 7 also reviews the existence of a period-four periodic orbit (the four separated bands) and a period-three periodic orbit at the tips of the triangular structure. We note the all orbits that exist in the triangular structure are stable orbits.

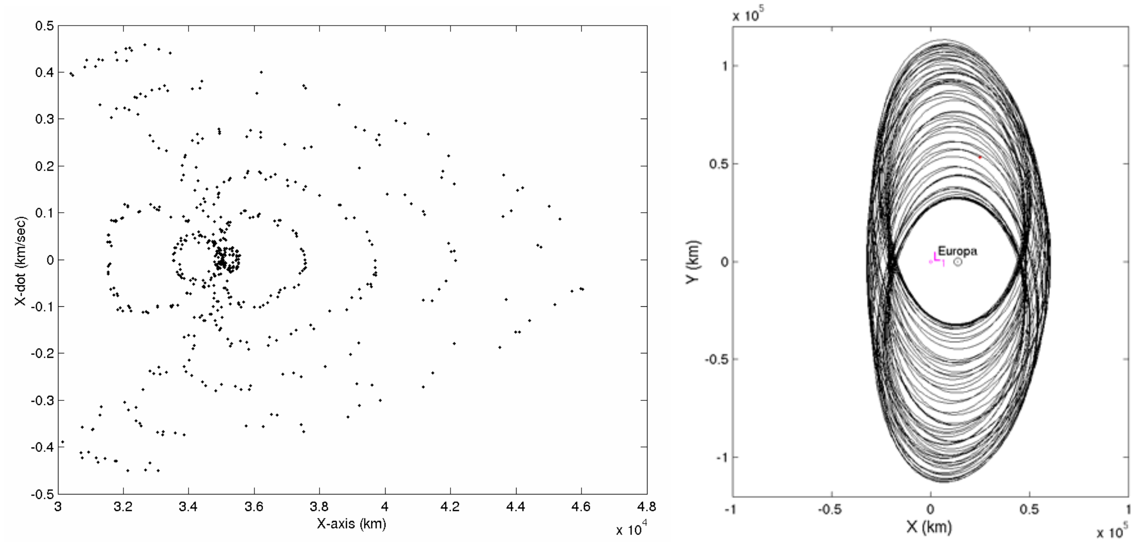

(a) **(b)**

Figure 8 (a) DROs with an initial X value at 35,000 km from Europa with varying velocity at the Y = 0 crossing (35,000 km corresponds to x = 1.76579 in Hill's units). Due to the current limitation of Mystic propagation to a few hundred days in this case, enough points to generate an apparent curve could not be generated, but the pattern is evident. Velocities are inertial values. (b) Quasi-periodic DRO representing the outer most curve in the Poincaré plot (left), X = 35,000 km and Vy = -0.816 km/sec. See Figure 1 for the "near" periodic 35,000 km DRO.

Due to the fact that orbits using the real ephemeris do not have constant Jacobi energy we will first attempt to analyze families of DROs with the same initial position but with varying velocities (thus, varying energy). Figure 8 shows a family of 35,000 km DROs with varying energy. The point (35000, 0) represents the near periodic DRO, curves to the right of the DRO represent librating DROs with larger energy and size, while the curves to the left of the DRO represent librating DROs with smaller energy and size. Figure 9 represents the same initial conditions in Figure 8 but uses Hill's equation. We note the "tail" in Figure 9 extends further than in Figure 8 signifying the existence of periodic and quasi-periodic orbits approaching very close to Europa in Hill's case. Using real ephemerides (Figure 8), these close approach orbits are not stable and quickly escape from Europa. Although this method allows us to view the existence of periodic and quasi-periodic orbits when using the ephemerides, it does not sufficiently allow one to view the stability of an entire family of orbits. In the next section we will describe a better approach in viewing stability, but the trade-off is the loss of the information about the orbit's periodicity.

STABILITY OF DROs

As stated in the introduction, DROs are desirable quarantine orbits because of their long-term stability. In analyzing stability of DROs in the real ephemeris it is beneficial to adopt Benest's method in viewing stability (Ref. 6) and Figure 10. This is because traditional stability diagrams for periodic and quasi-periodic orbits usually depict stability for a fixed Jacobi constant, but due to the lack of a constant for the Jacobi integral using the real ephemeris we will depict stability using Benest's method. Benest's method requires something similar to the Poincaré section in Figures 7-9. Benest's method considers the Y velocity of the DRO as the orbit crosses the XZ-plane in the rotating coordinate system. If we were to sample DROs every time they cross the XZ-plane on the positive X-axis (away from Jupiter), then for the periodic orbits, or near periodic orbits, we would see a "dot" representing the trajectory in the (V_Y, X) Poincaré section. If we are to look at the entire family of DROs, then a curve such as the dotted curve in Figure 10, will emerge. Since the orbits are in the retrograde direction and we are looking at the positive X-axis crossing, then the velocity in the Y direction is negative, $V_Y < 0$.

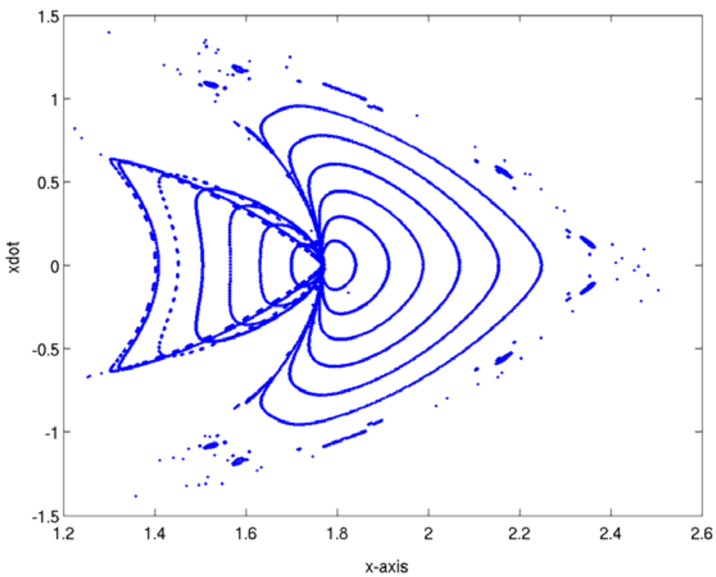

Figure 9 Similar to Figure 8: analytical propagation of the Poincaré sections for x = 35,000 km DROs with various energy levels. Axes are in Hill's units. Note that the orbits toward the left of the periodic 35,000 km DRO extends much closer to Europa then that of the real ephemeris.

Figure 10 depicts the stability limits of quasi-periodic or librating DROs (thicker solid lines). The two solid lines are the minimum and maximum velocities a DRO, at a distance X away, can have before it escapes in 200 days. Regions outside of the bounds are labeled as "unstable". Although not plotted on Figure 10, the velocity profile close to Europa (less then 5,000 km) closely matches that of a circular orbit. Unlike circular orbits, where the velocity decreases as a function of distance from the body, the velocity profile for the DROs diverges from the circular velocity profile and increases as a function of distance. The DRO velocity requirement rises linearly beyond approximately 2 times the distance to L1, see Figure 11.

From Figure 10 and 11, we note that with the exception for three specific points on the stability curve, the DROs are *all* stable for at least 200 days. Two of the cases where the stability bounds merge together (near the 5:2 and 4:3 resonances) correspond to the intersection of the unstable family of triple-periodic orbits *g3* (Figure 3). The resonance where these instability "necks" occurs differ between the ephemeris case and Hill's case. These two specific cases of instability for DROs, and the family *f* orbits in general, were investigated in detail by Henon and Benest (Ref. 1 thru 6). These instabilities appear for all of the Galilean moons. The instability region near the resonance 3:2 seems to appear only for Europa's case. This third instability region creates a third region around Europa where DROs should not be used as quarantine orbits.

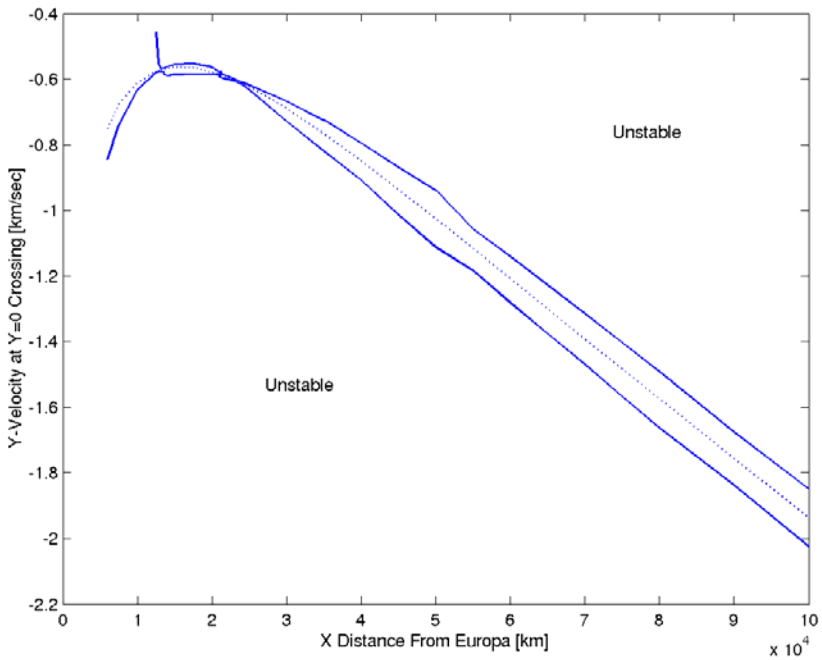

Figure 10 Stability diagram for Europa's family of DROs in the ephemeris model. Dotted lines represents the "near" periodic DROs, while the solid thicker curves represents the minimum and maximum velocities, before escape is un-avoidable. Stability, in this plot is defined by an orbit not escaping Europa or colliding with Europa for at least 200 days. Velocities are inertial values.

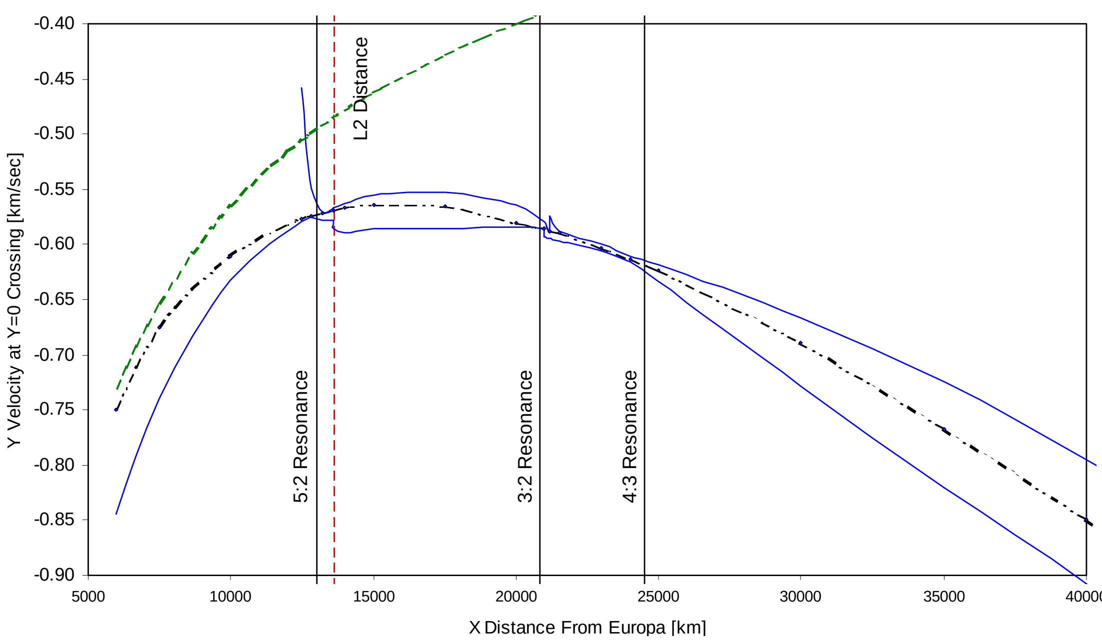

Figure 11 Enlargement of Figure 10 with resonances relative to Europa marked. Note the sensitive regions where DROs become very unstable. Key: -..-..- "near" periodic DROs, ---- stability bounds for the DROs, and - - - velocity profile for a two-body circular orbit.

Another benefit of this method of depicting stability for DROs is that one can also use the plot as a guide to initial conditions for any size DROs. For targeting purposes you will only need a coordinate transformation to align your X-axis along the Jupiter-Europa line and Figures 10 & 11 will give the necessary position and velocity state to obtain a DRO ($Y = 0$, $V_X = 0$).

Out-of-Plane DROs

Thus far, we have only looked at near planar DROs, or in Hill's case, exactly planar DROs, but Hénon showed that stability is not limited to the planar case (Ref. 13 & 14). Again, in viewing stability for the restricted three-body problem it is usually ideal to express stability in terms of a Jacobi constant, but using the ephemeris model we must take another approach. In order to analyze the stability of a DRO in three-dimensional space, we first began by looking at a planar DRO and observe its stability when we add a Z-component to the velocity. Figure 12a indicates the stability of a 35,000 km DRO (measured along the X-axis). We note from Figure 12b-d that an out-of-plane DRO is similar in shape to a Lissajous orbit about L1 or L2. Again, taking the right X-axis crossing of the XZ-plane, we note the Y-velocity and the Z-velocity at the crossing that bounds the DRO for at least 200 days, which we define as stable. Figure 13 shows the stability profile for the 11,000 km and the 13,200 km Europa DRO propagated for 100 days. Note the decrease in the area of the stable region as we approach the instability "neck" (visible in Figure 11) at about 13,500 km from Europa.

If one generates the entire vertical stability diagram for the family of DROs, then a third (V_Z) axis could be added to Figure 11 and 12, and stability "tube" of initial conditions for the DROs develops (Figure 14 represents a single cross section of the tube). A benefit arises from the stability of out-of-plane DROs: we can target out-of-plane DROs and potentially save plane change ΔVs depending on initial or final desired inclinations.

We have not fully investigated the stability of quasi-periodic DROs because we have neglected several other dimensions. By adding a Vz axis to Figure 10 and 11, we are still neglecting the Vx-

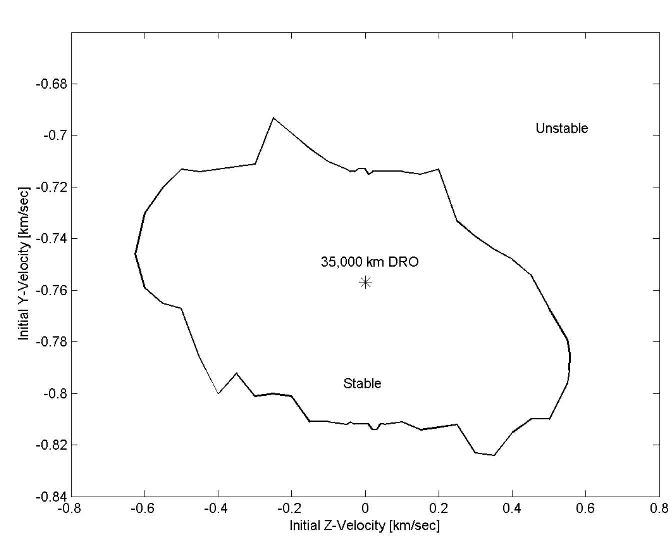

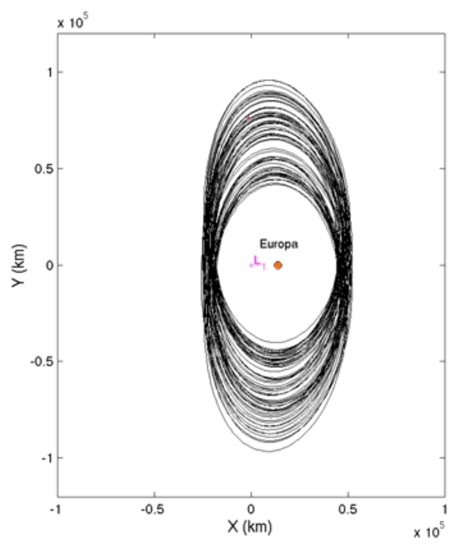

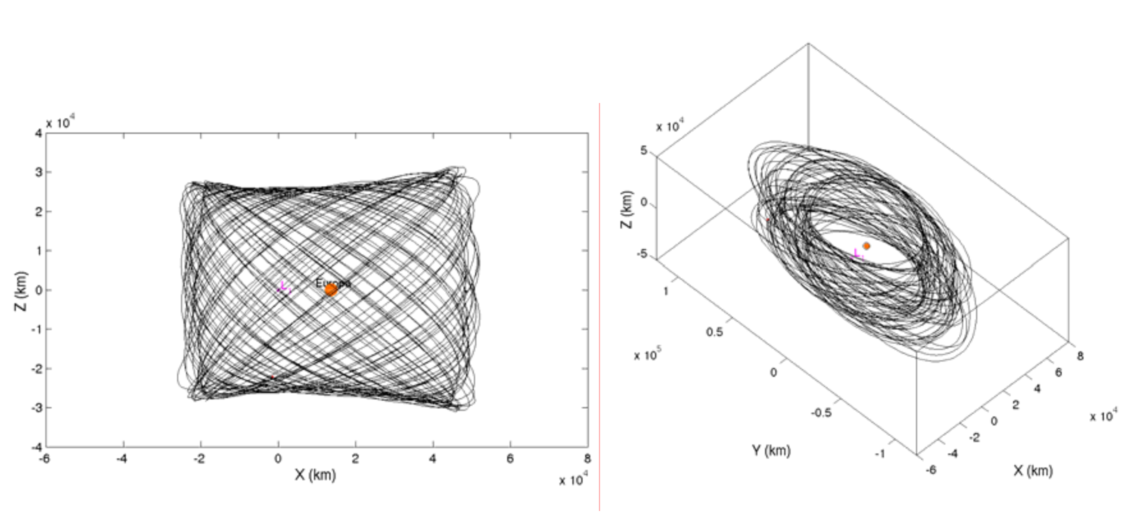

Figure 13 (a) Stability profile for 35,000 km out-of-plane DRO (Europa). A "slice" of Figure 12 stability diagram at X = 35,000 km. The asterisk (*) represents the conditions for a planar "near" periodic DRO. (b) Example of a 35,000 km out-of-plane DRO in the XY-frame with V_Y = -0.767 km/sec and V_Z = -0.55 km/sec, (c) in the XZ-frame, and (d) in the XYZ-view. Propagated for 200 days. Jupiter-Europa L1-centered. Velocities are inertial values.

dimension and the Z-dimension, because we assume that the orbit crosses the rotating x-axis with Vx = 0 at Y = 0. To obtain some understanding of the 6-dimensional problem, we analyzed the stability of periodic DROs by rotating the velocity vector of the DROs at the right crossing of the rotating x-axis. This method gives rise to the "Red Sea" Plot (Figure 14). Figure 14 shows the stability of retrograde orbits at various "inclinations" or velocity rotation angles created by rotating the planar periodic DROs' velocity out of the X-Y plane. The blue area represents orbits which are stable for at least 100 days. One key observation is the sharp division or "cliff" between stable orbits and unstable orbits, which is a characteristic of DROs (although not shown similar cliffs occur for Figure 10 thru 13). The "cliff" remains in a similar location even when the test for stability is extended to 1,000-year propagations.

The presence of the blue region in Figure 14 indicates the existence of a continuous family of three-dimensional DROs using the real ephemeris from very large radii to small radii around Europa. This implies the existence of stable pathways accessible to low-thrust vehicles that allow transfers over a large

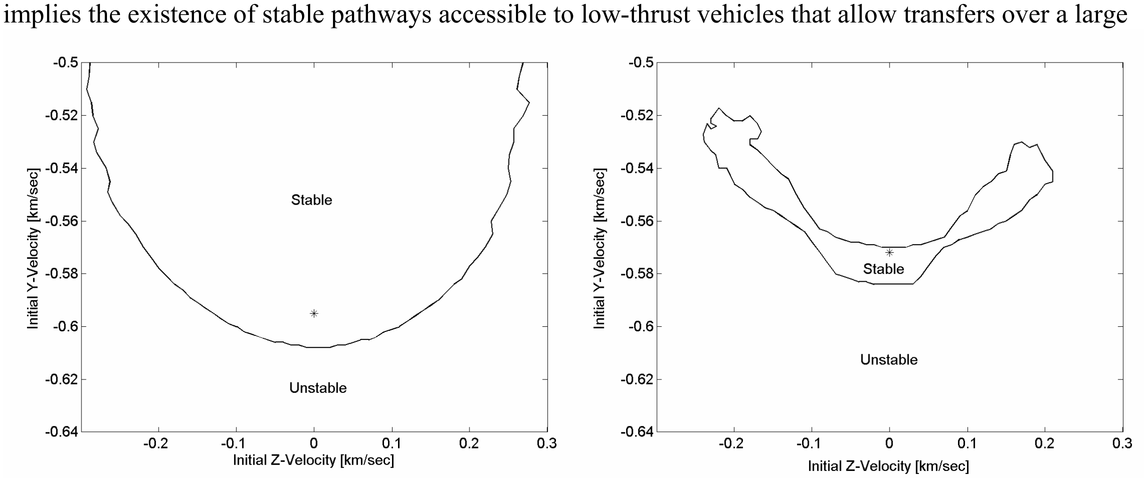

(a) **(b)**

Figure 13 (a) Stability profile for 11,000 km out-of-plane DRO (Europa). A slice of Figure 11 stability diagram at X = 11,000 km. The asterisk (*) represents the conditions for a planar "near" periodic DRO. (b) Stability profile for 13,200 km out-of-plane DRO near the instability "neck" region.

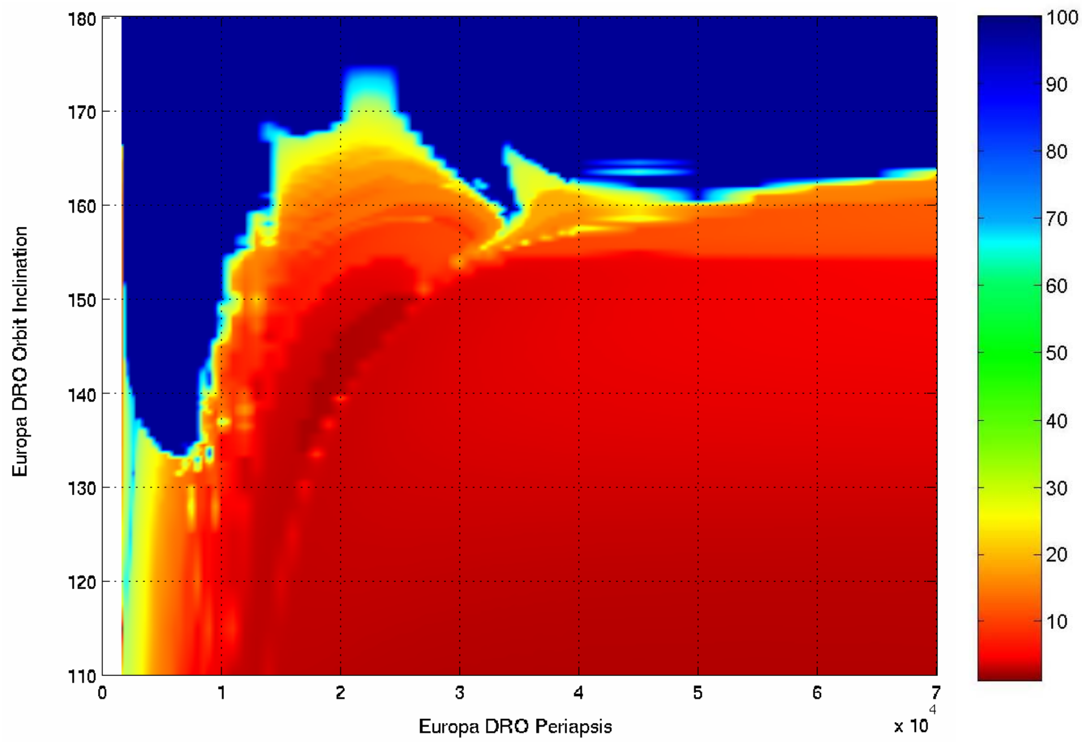

Figure 14 The "Red Sea Plot" depicts stability of periodic DROs as a function of inclination (in degrees) and distance along the rotating x-axis (in kilometers). The colorbar scale indicates orbital lifetime in days.

range of radii and inclinations. This is a significant result because the feasibility of designing low-thrust missions to orbit Europa may require instantaneous stability during transfers. The captured phase space around Europa is generally very treacherous; if thrust control is lost for as little as two days, impact or escape from Europa can be unavoidable. It should be noted that the stability diagram (Figure 14) is somewhat conservative because orbital lifetime may be increased by varying the magnitude of the velocity vector (which was only rotated to produce the inclination).

TRANSFERS TO AND FROM DROs

Transfer trajectories to DROs have been investigated by Hénon, Ocampo and Rosborough, and Kechichian, et al. By using what Ocampo calls Earth-Return periodic Orbits (EROs) for DROs about Earth or what Hénon refers to as the asymptotic cases for a (and/or c) and g', these orbits can be used as initial reference state for transfer trajectories to DROs (DRO Transfer Orbits – DTO) (Ref. 11, 12, & 15). Impulsive transfers can be accomplished by "hopping on" to periodic orbits, such as the Lyapunov orbits in Figure 6. In the case of low-thrust transfers, it is necessary to have enough thrust-to-mass to safely control the spacecraft. This requirement can be reduced by finding instantaneously stable or near stable transfers. Figure 14 suggests pathways between DROs, however, transfers from non-DRO states to DROs will typically require passage through orbital states that result in Europa impact if spacecraft control is lost for even short period of times.

Impulsive Transfers between DROs and Low Altitude Orbits

A direct transfer from a prograde (inclination at 0°) low altitude orbit around Europa to a DRO is to use a Lyapunov transfer orbit. Recall that in the asymptotic case family a orbits (which originate from

L_2) approach Europa at very close distances, as seen in Figure 6 and 15. These orbits are retrograde orbits about L_2 in the rotating frame, but relative to Europa these orbits are prograde at close approaches and are retrograde relative to Europa at greater distances. It is clear that large family *a* orbits resemble the shape of DROs at the outermost most distances, and can be use as transfer points where DROs and family *a* orbits are tangent at the X-axis crossing. This geometric approach is much like a Hohmann transfer, where ΔV_1 is applied at the low science orbit when it is tangent to a family *a* orbit at the crossing of the Jupiter-Europa plane. ΔV_2 will then be applied at a half-period later, again at the crossing of the Jupiter-Europa line where

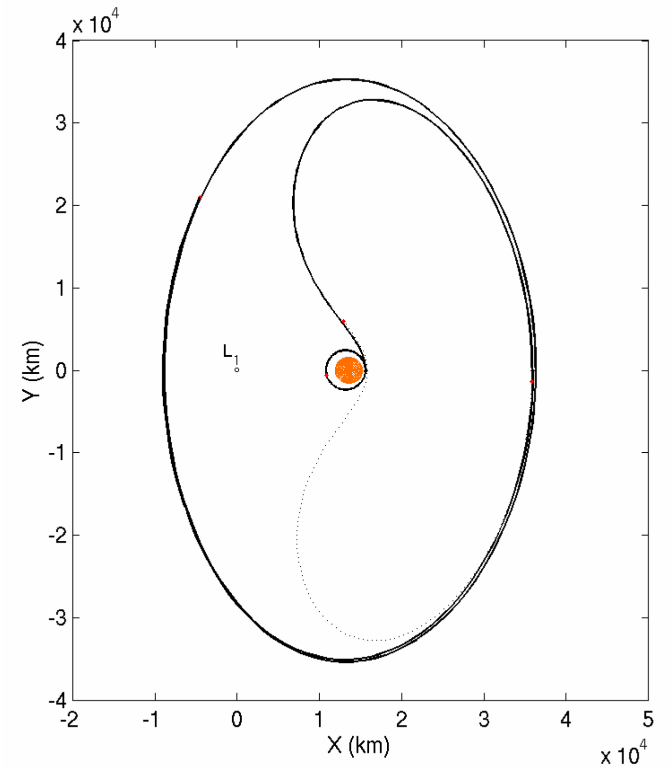

Figure 15 Impulsive transfer from a circular 600 km altitude parking orbit at 0° around Europa to a 20,000 km (x-axis) DRO. Impulsive ΔV = 0.596 km/sec for the transfer.

the DRO and the family *a* orbit are tangent, see Figure 15. This type of transfer was investigated numerically by Ocampo and Rosborough (Ref. 11) for transfer trajectories from Earth LEO to DROs. Ocampo and Rosborough called these transfers "Class-A ERO" having only 2 crossing of the X-axis during the transfer. A similar family of Lyapunov orbits exist around L_1, and can be used to transfer between the DRO and the low altitude orbit.

Following Ocampo's nomenclature, Class-B EROs are transfer trajectories that have the asymptotic form of family *g'*, consisting 4 crossings of the x-axis (dotted lines on Figure 16a), and Class-C EROs with 8 crossings of the x-axis (dotted lines on Figure 16b). Ocampo has also shown that the difference in ΔV between the Class A and C diminishes to zero for large DROs, but the transfer time for C is nearly three times as long. Ocampo also noted that for his test runs, Class-B transfers are the least preferable in terms of ΔV due to the large difference in the Jacobi constant between the transfer orbit and the DROs (Ref. 11).

Low Thrust Transfers

Due to the strong third body effects from Jupiter and the small mass of Europa, low thrust transfers can be tricky to design. Since the Mystic tool takes into account N-bodies, many periodic orbits cease to exist due to perturbations. This is evident by an oscillation in the Jacobi constant (Figure 17), which is usually used to define a periodic orbit in three-body problems. Targeting a (near) periodic orbit using a real ephemeris is not simple. This section will present some preliminary findings on low-thrust transfers between a low-altitude, inclined science orbit around Europa and a DRO.

Spiral Outs to and from DROs. The simplest case of a transfer out to a DRO and a transfer from a DRO to Europa Science Orbit for low thrust systems is to thrust along and against the inertial velocity vector, respectively. A spiral-out from a small retrograde circular orbit (radius < 6,000 km) around Europa can be achieved with a simple continuous burn along the velocity vector of the transfer, assuming the initial orbit is a circular orbit with an inclination of 180° and a thrust acceleration of < 0.5 mm/s^2. The result of this

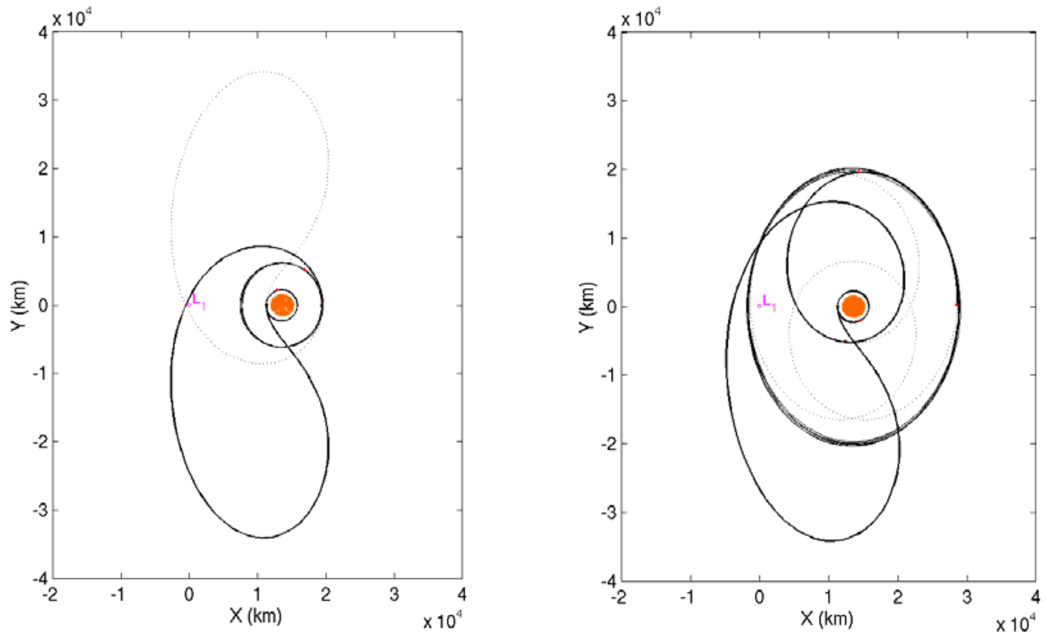

(a) (b)

Figure 16 (a) Class B impulsive transfer from a circular 600 km altitude parking orbit at 0° around Europa to a 6,000 km (x-axis) DRO. Class B impulsive ΔV = 0.343 km/sec for the transfer. (b) Class C Class impulsive transfer to a 15,000 km (x-axis) DRO. Class B impulsive ΔV = 0.566 km/sec for the transfer.

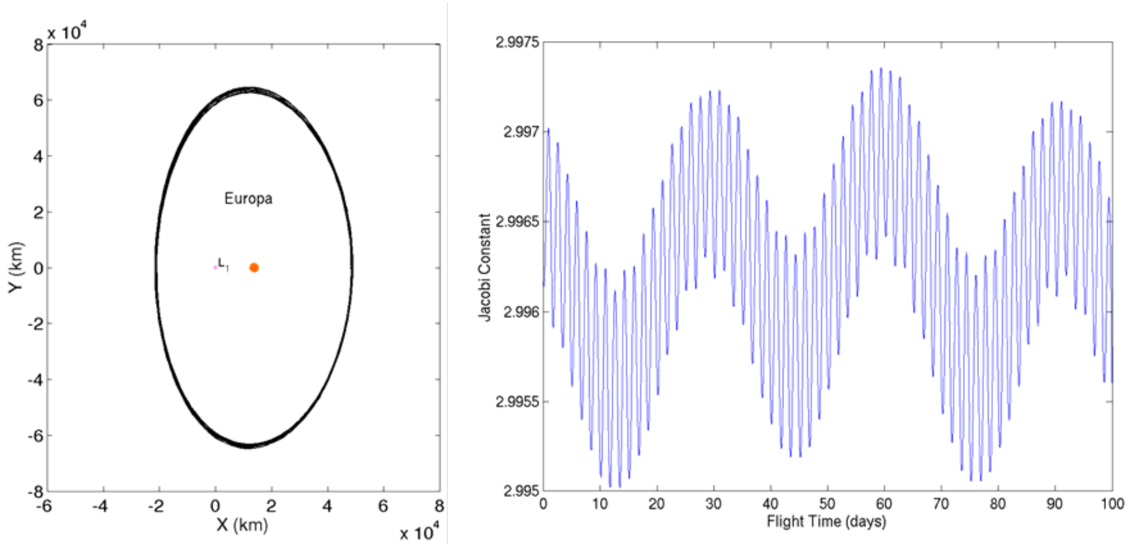

(a) **(b)**

Figure 17 (a) Europa's "near" planar 35,000 km DRO. (b) Oscillation of the Jacobi Constant as a function of time. Time = 0 days corresponds to X = 35,000 km and Y = 0 at the DRO. The smaller period oscillation in the Jacobi Constant is half that of a DRO period in the rotating frame.

transfer will be a DRO at the end of the burn. Here, we ignore the plane change required to go from an inclined science orbit to a planar DRO orbit. If the thrust-to-mass ratio remains low during the transfer then the transfer remains in the DRO family in phase space. In other words, the spiral out is continuously transferring to larger and larger DROs. The stability of the transfer can be visualized in Figure 18. Figure 19a, presents the spiral-out of a low thrust-to-mass ratio spacecraft (accel. = 0.1915 mm/s^2). The spiral-out follows the profile of a family of DROs. As a result, the spacecraft can shut thrusting off at any point along the transfer and be on a DRO. Although the transfer is not optimal, it provides a safe transfer. A transfer does not have to follow the DRO profile exactly to end up in a DRO, but for a safe transfer, it should always lie inside the stability region. Difficulties arise when plane changes are involved and the starting spiral-out radius is greater then 6,000 km. For spiral-outs starting at distances greater then 6,000 km the energy of the orbit is different from that of the nearby DROs and hence maneuvers are required to get to the DRO profile (See Figure 10 and Figure 18b).

To visualize why a simple spiral-out would result in DROs we plot the Y-component of the velocity in rotating frame as the trajectory crosses the XZ-plane on the right of Europa. Overlaying these values to that of the stability diagram (Figure 10 and 11) for Europa's family of DROs we can see the progression of the transfer as it spirals out. This view in phase space shows the transfer following the profile of the DROs, which explains how spiraling out can lead into a DRO. For cases where the transfer falls off the DRO profile (such as in Figure 19 for a spiral-out beginning with a 155 deg inclination instead of 180 deg inclination) it becomes necessary to perform maneuvers to target back to the DRO's profile. If the acceleration exceeds 0.5 mm/s^{2,} then the method of transferring between DROs by thrusting along the velocity vector will fail because the spacecraft's acceleration is large enough to escape the stability of a DRO and place it outside the bounds of Figure 18b.

Out-Of-Plane Spiral Ins and Outs to DROs. Spiral-in and -out transfers are not limited to in-plane transfers. Analysis has shown that by spiraling out at inclinations as high as 145 degrees one can get into a DRO. For higher inclinations, the region of obtainable DRO sizes decreases. This can be explained from viewing Figure 19. The general trend for spiral-outs at various inclinations is that the higher the initial inclination the more the profile shifts away from the DRO profile. For an initial inclination of 155 degrees (Figure 19), if the engine were to shut off at any point between the distances of 15,000 km and

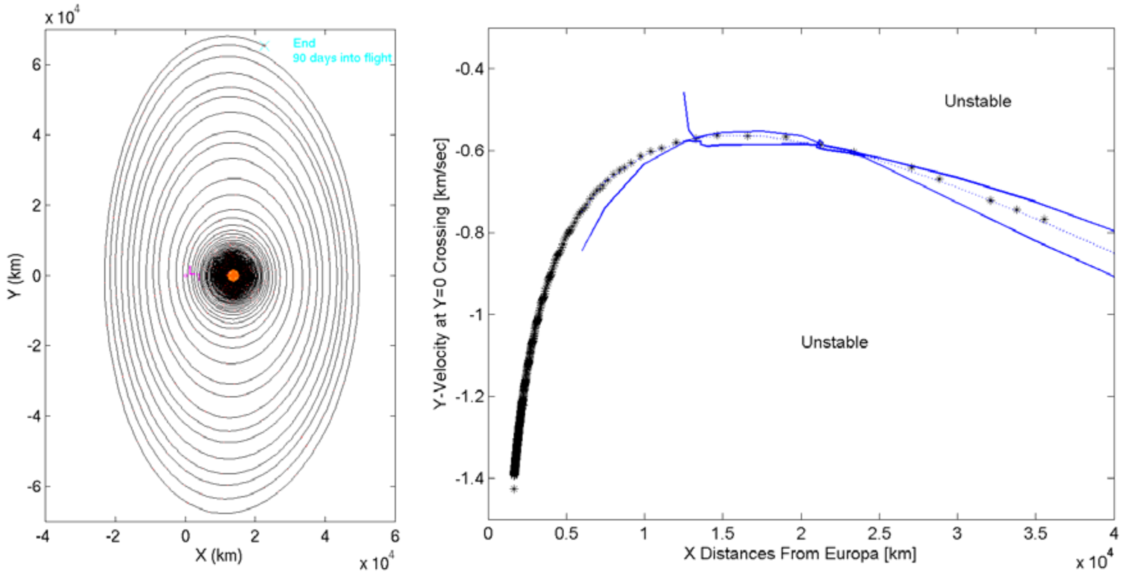

(a) **(b)**

Figure 18 (a) Spiral-out transfer from a 100 km (altitude) retrograde (i=180 deg) circular orbit. Burn time of 90 days with an acceleration = 0.1915 mm/s^2. Note that the spiraling produces concentric DRO orbits. This characteristic of spiraling out exists for nearly all thrust-to-mass ratios up to about 0.4 mm/s^2. (b) Phase space plot of the right Y crossing velocity of the XZ-plane, * denotes crossing points. Note that the spiraling out transfer follows the profile of the DRO family.

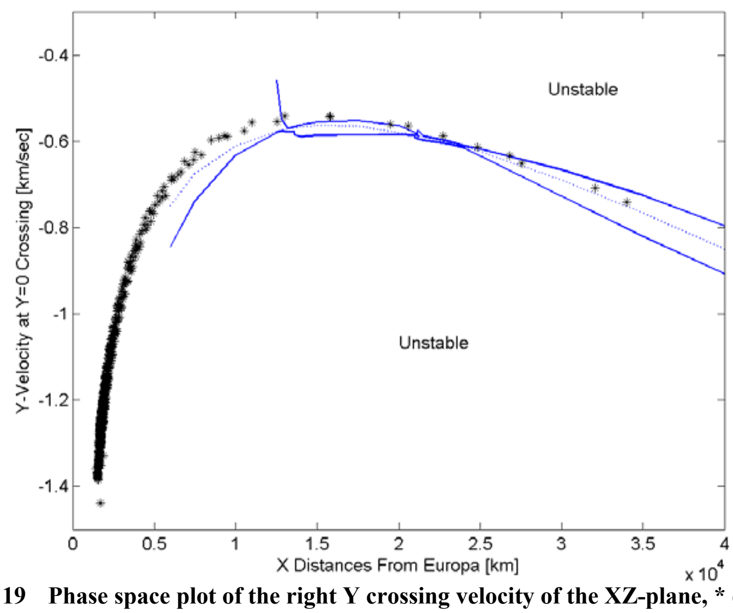

Figure 19 Phase space plot of the right Y crossing velocity of the XZ-plane, * denotes crossing points. Transfer from a 100 km (altitude) circular orbit at 155 degrees inclination. Burn time of 90 days with an acceleration = 0.1915 mm/s^2. Note that the profile of spiraling out transfer is shifted in comparison to Figure 18b.

23,000 km on the X-axis, then the spacecraft can escape. If the transfer proceeds past the regions where the stability bounds merge, then the spacecraft will again be inside the stable DRO region. In cases where the transfer profile shifts too high above the curve, (for example when the initial inclination is 140 degrees), the profile will never re-enter the stable DRO region.

Transfer to and from DROs with Plane Changes. Our transfers assume a circular science orbit at 100 km altitude with an inclination of 110°. We do not take into account Europa's gravitational harmonics in this analysis. Transfers from the Europa science orbit to a 35,000 km planar DRO were computed using Mystic trajectory optimization software. The data is represented on Figure 20. The data is for fairly high acceleration (accel. > 0.3 mm/s^2) transfers. Figure 21 represents optimized transfers from a 35,000 km planar DRO to a circular 5,000 km orbit at 125°. In both Figures, the transfers are not always instantaneously stable transfers. We found that transfers that have many coast arcs (long flight times) can be very unstable. Recall from Figure 14 (the "Red Sea" plot) that for inclinations between 110° to ~ 135° there are regions of very low lifetime, and to transfer to the science orbit there is no obvious way to avoid the unstable regions. But Figure 14 does show that by using the DRO profile, one can safely transfer continuously between low altitude orbits (~5,000 km) with a range of inclinations (180° to ~135°) and very distant orbits.

DRO Type Escapes and Captures. If one desires to escape a body with a high V_∞, DROs act much like a "coiled spring" to achieve this goal. A spacecraft can achieve a larger departure V_∞, by swinging by Europa after departing from a large DRO (Ref. 19). Unlike many other types of orbits (i.e. Distant Prograde Orbits) which can also produce such high velocities or energies, DROs are stable. Because they are simple-periodic and near elliptical in shape they are much less chaotic to control and design. This build-up of energy is due to the DROs high velocity relative to Europa, which are many times faster then two-body circular orbits and Lyapunov orbits of the same size (recall Figure 11). Whiffen refers to these

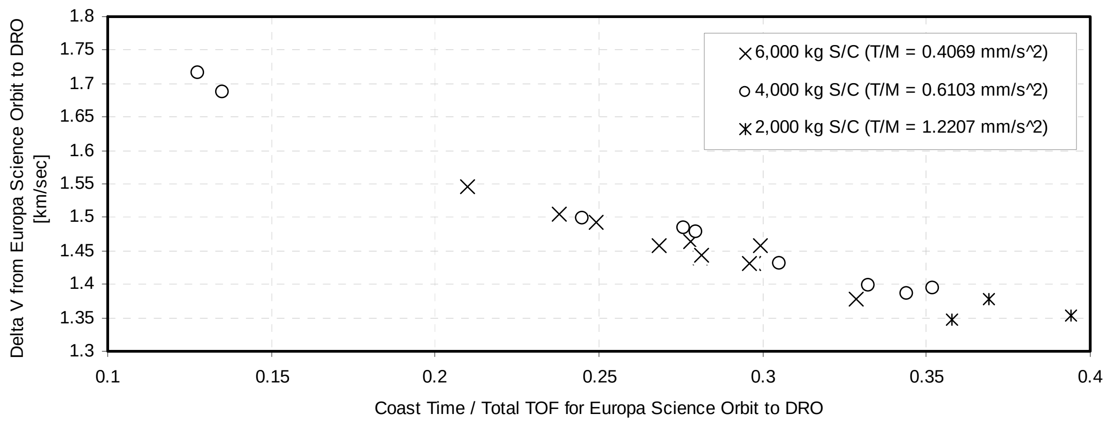

Figure 20 Optimized transfers from a Europa's science orbit (100 km altitude at 110°) to a 35,000 km planar DRO.

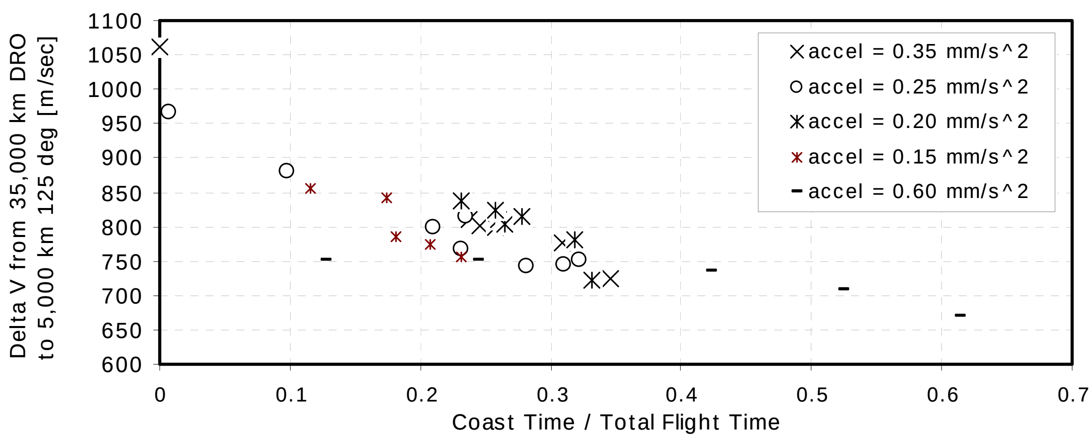

Figure 21 Optimized transfers from a 35,000 km planar DRO to a 5,000 km circular obit at 125° around Europa.

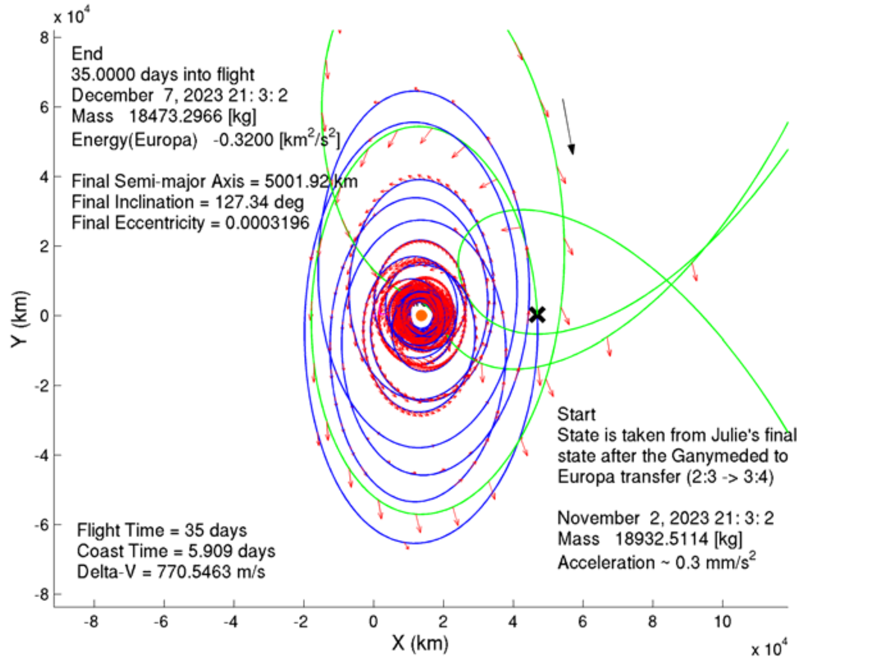

Figure 22 DRO-Type Capture in green. Optimize transfers from a 30,000 km DRO at 175° to a 5,000 km circular obit at 125° around Europa in blue. Flight time and ΔV noted on the plot are for the final (blue) transfer down to Europa.

transfers as DRO-type escapes (Ref. 18).

The DRO type escape can be reversed to achieve a very efficient capture. If one desires a safe transfer down to Europa, then capturing at a DRO may be more beneficial than capturing along the stable manifold of an L2 Halo orbit. If time is an issue, then a DRO type of capture *may* not be beneficial due to the extended time required to spiral-down from such a distant orbit. The trade issues between orbital safety, time, ΔV, and capture/escape types are numerous and are currently being studied. See Whiffen (Ref. 18) for a brief discussion on capture and escape types. Figure 22 is an example of a capture/spiral transfer that uses many of the elements discussed in this paper. The transfer exploits a DRO-type of capture. Figure 22 shows the capture portion in green which was generated by Julie Kangas. The transfer in blue is the spiral-in portion from 30,000 km at 175° inclination to a circular orbit at 5,000 km and 125° inclination.

CONCLUSION AND FUTURE WORK

Distant Retrograde Orbits are among the most stable periodic orbits in any system with third-body perturbations. DROs can play an important role in designing safe transfers to and from Europa and in designing quarantine orbits. The research done in this paper can be extended to many other multi-body systems. Although much is already known about DROs, further research are needed to better understand out-of-plane DROs and understand how to utilize them for safe transfers to and from Europa. These tasks are currently underway.

ACKNOWLEDGMENTS

The authors would like to thank M. Hénon for answering our email questions, C. Ocampo for providing a copy of his thesis, Jon Sims for giving us the opportunity to explore these interesting orbits, Ryan Russell for his contribution to the stability of DROs, and Julie Kangas for providing us a Ganymede to Europa transfer. The research described in this paper was carried out at the Jet Propulsion Laboratory, California Institute of Technology, under contract with the National Aeronautics and Space Administration.

REFERENCES

1. Hénon, M., “Numerical Exploration of the Restricted Problem V. Hill’s Case: Periodic Orbits and Their Stability” Astronomy & Astrophysics, Vol. 1, 223-238 (1969).

2. Hénon, M., “Numerical Exploration of the Restricted Problem VI. Hill’s Case: Non-Periodic” Astronomy & Astrophysics, Vol. 9, 24-36 (1970).

3. Benest, D., “Effects of the Mass Ratio on the Existence of Retrograde Satellites in the Circular Plane Restricted Problem IV. Three-dimensional Stability of Plane Periodic Orbits” Astronomy & Astrophysics, Vol. 54, 563-568 (1976).

4. Brouke, R.A., “Periodic Orbits in the Restricted Three-Body Problem With Earth-Moon Masses,” Technical Report 32-1168, Jet Propulsion Laboratory, California Institute of Technology (1968).

5. Benest, D., “Effects of the Mass Ratio on the Existence of Retrograde Satellites in the Circular Plane Restricted Problem” Astronomy & Astrophysics, Vol. 32, 39-46 (1974).

6. Benest, D., “Effects of the Mass Ratio on the Existence of Retrograde Satellites in the Circular Plane Restricted Problem. II” Astronomy & Astrophysics, Vol. 45, 353-363 (1975).

7. Whiffen, Gregory J., and Sims, Jon A., “Application of a Novel Optimal Control Algorithm to Low-Thrust Trajectory Optimization,” Paper AAS 01-209, AAS/AIAA Astrodynamics Specialist Conference, Santa Barbara, California, February 11-14, 2001.

8. Szebehely, V., *Theory of Orbits in the Restricted Problem of Three Bodies*, Academic Press, Inc. 1967.

9. Scheeres, D.J., M.D. Guman and B. Villac, “Stability Analysis of Planetary Satellite Orbiters: Application to the Europa Orbiter,” Journal of Guidance, Control, and Dynamics 24(2): 778-787, 2001.

10. Hénon, M., *Generating Families in the Restricted Three-Body Problem*, Lecture note in physics, Springer-Verlag Berlin Heidelberg (1997).

11. Ocampo, C. A., and Rosborough, G. W., “Transfer Trajectory for Distant Retrograde Orbiters of the Earth”, AAS 93-180, AAS/AIAA Spaceflight Mechanics Meeting, Pasadena, CA, 22-24 February 1993.

12. Ocampo, C. A., and Rosborough, G. W., “Optimal Low-Thrust Transfers Between a Class of Restricted Three-Body Trajectories”, AAS 93-681, Advances in the Astronatical Science, Vol. 85, Part II (1994).

13. Hénon, M., “Vertical Stability of Periodic Orbits in the Restricted Problem I. Equal Masses” Astronomy & Astrophysics, Vol. 28, 415-426 (1973).

14. Hénon, M., “Vertical Stability of Periodic Orbits in the Restricted Problem II. Hill’s Case” Astronomy & Astrophysics, Vol. 30, 317-321 (1974).

15. Kechichian, J.A. et al., “Solar Surveillance Zone Population Strategies with Picosatellites Using Halo and Distant Retrograde Orbits” 7th International Conference on Libration Point Orbits and Application, Parador d’Aiguablava, Spain, 10-14 (2002).

16. Benest, D., “Libration Effects for Retrograde Satellites in the Restricted Three-Body Problem I: Circular Plane Hill’s Case” Celestial Mechanics, Vol. 13, 203-215 (1976).

17. Benest, D., “Effects of the Mass Ratio on the Existence of Retrograde Satellites in the Circular Plane Restricted Problem. III” Astronomy & Astrophysics, Vol. 53, 231-236 (1976).

18. Whiffen, Gregory J., “An Investigation of a Jupiter Galilean Moon Orbiter Trajectory”, Paper AAS 03-544, AAS/AIAA Astrodynamics Specialist Conference, Big Sky, Montana, August 3-7, 2003.